doi:10.1093/brain/awu339 BRAIN 2015: 138; 371–387 | 371

BRAIN
A JOURNAL OF NEUROLOGY

Targeting pharmacoresistant epilepsy and epileptogenesis with a dual-purpose antiepileptic drug

Anna Doeser,[1,*] Gesa Dickhof,[1,*] Margit Reitze,[1] Mischa Uebachs,[1,2] Christina Schaub,[1,2] Nuno Miguel Pires,[3] Maria João Bonifácio,[3] Patrício Soares-da-Silva[3,4] and Heinz Beck[1,5]

*These authors contributed equally to this work.

See Lerche (doi:10.1093/awu357) for a scientific commentary on this article.

In human epilepsy, pharmacoresistance to antiepileptic drug therapy is a major problem affecting a substantial fraction of patients. Many of the currently available antiepileptic drugs target voltage-gated sodium channels, leading to a rate-dependent suppression of neuronal discharge. A loss of use-dependent block has emerged as a potential cellular mechanism of pharmacoresistance for anticonvulsants acting on voltage-gated sodium channels. There is a need both for compounds that overcome this resistance mechanism and for novel drugs that inhibit the process of epileptogenesis. We show that eslicarbazepine acetate, a once-daily antiepileptic drug, may constitute a candidate compound that addresses both issues. Eslicarbazepine acetate is converted extensively to eslicarbazepine after oral administration. We have first tested using patch-clamp recording in human and rat hippocampal slices if eslicarbazepine, the major active metabolite of eslicarbazepine acetate, shows maintained activity in chronically epileptic tissue. We show that eslicarbazepine exhibits maintained use-dependent blocking effects both in human and experimental epilepsy with significant add-on effects to carbamazepine in human epilepsy. Second, we show that eslicarbazepine acetate also inhibits $Ca_v3.2$ T-type Ca^{2+} channels, which have been shown to be key mediators of epileptogenesis. We then examined if transitory administration of eslicarbazepine acetate (once daily for 6 weeks, 150 mg/kg or 300 mg/kg) after induction of epilepsy in mice has an effect on the development of chronic seizures and neuropathological correlates of chronic epilepsy. We found that eslicarbazepine acetate exhibits strong antiepileptogenic effects in experimental epilepsy. EEG monitoring showed that transitory eslicarbazepine acetate treatment resulted in a significant decrease in seizure activity at the chronic state, 8 weeks after the end of treatment. Moreover, eslicarbazepine acetate treatment resulted in a significant decrease in mossy fibre sprouting into the inner molecular layer of pilocarpine-injected mice, as detected by Timm staining. In addition, epileptic animals treated with 150 mg/kg, but not those that received 300 mg/kg eslicarbazepine acetate showed an attenuated neuronal loss. These results indicate that eslicarbazepine potentially overcomes a cellular resistance mechanism to conventional antiepileptic drugs and at the same time constitutes a potent antiepileptogenic agent.

1 Laboratory for Experimental Epileptology and Cognition Research, Department of Epileptology, University of Bonn, Sigmund-Freud-Straße 25, 53105 Bonn, Germany
2 Department of Neurology, University of Bonn, Bonn, Germany
3 BIAL – Portela & C[a], S.A., S. Mamede do Coronado, Portugal
4 MedInUP – Center for Drug Discovery and Innovative Medicines, University of Porto, Porto, Portugal
5 German Center for Neurodegenerative Diseases (DZNE), Ludwig-Erhard-Allee 2, 53175 Bonn, Germany

Correspondence to: Heinz Beck,
Laboratory for Cognition Research and Experimental Epileptology,
Department of Epileptology,

Received June 9, 2014. Revised September 30, 2014. Accepted October 5, 2014. Advance Access publication December 3, 2014

University of Bonn,
Sigmund-Freud Str. 25,
53105 Bonn, Germany
E-mail: Heinz.beck@ukb.uni-bonn.de

Keywords: pharmacoresistance; epilepsy; anticonvulsant drugs; antiepileptogenesis; eslicarbazepine

Abbreviations: CBZ = carbamazepine; ESL = eslicarbazepine acetate; I_{NaP} = persistent Na^+ current; I_{NaT} = transient Na^+ current; OXC = oxcarbazepine; TLE = temporal lobe epilepsy

Introduction

In human epilepsy, pharmacoresistance to anticonvulsant drug therapy is a major problem affecting a substantial fraction of patients. Many of the currently available anticonvulsant drugs target voltage-gated sodium channels, leading to a rate-dependent suppression of neuronal discharge (Köhling, 2002). This feature of sodium channel blocking anticonvulsant drugs is thought to be responsible for their efficacy in blocking high-frequency aberrant neuronal activity during seizures. In patients with chronic refractory temporal lobe epilepsy (TLE), experiments on hippocampal tissue obtained during epilepsy surgery have shown that use-dependent block of voltage-gated sodium channels by carbamazepine (CBZ) is strongly reduced. Parallel experiments in the pilocarpine model of experimental epilepsy confirmed that acquired epilepsy in an animal model can also be associated with a loss of use-dependent block by CBZ (Remy *et al.*, 2003*a*, *b*). The molecular mechanisms leading to altered pharmacosensitivity of neuronal sodium channels are so far unknown (Uebachs *et al.*, 2010). Nevertheless, the loss of a potential cellular mechanism of action in both patients and experimental epilepsy suggests that loss of use-dependent block may be a cellular mechanism of pharmacoresistance in chronic epilepsy. It would be highly desirable to identify sodium channel blockers that overcome the loss of efficacy demonstrated for CBZ in chronically epileptic tissue. New sodium channel acting anticonvulsants such as eslicarbazepine acetate (ESL) seem to show additional clinical benefit (Elger *et al.*, 2007, 2009; Ben-Menachem *et al.*, 2010; Halász *et al.*, 2010), suggesting that they might not exhibit the same resistance mechanism.

Apart from the development of pharmacoresistance, a further major unsolved problem in the treatment of epilepsy is the lack of compounds that can be clinically used to inhibit the progression of epilepsy. This process has been termed epileptogenesis. So far, a number of experimental studies have shown positive treatment effects on epileptogenesis (Löscher and Brandt, 2010; Pitkänen, 2010; Pitkänen and Lukasiuk, 2011; Jimenez-Mateos *et al.*, 2012). However, there are, to our knowledge, no candidate compounds available that could be introduced into a clinical study.

In this study, we have investigated eslicarbazepine, the major active metabolite of ESL, and have studied both its efficacy in human and experimental epilepsy and its efficacy in blocking epileptogenesis. Our results show that eslicarbazepine exhibits maintained use-dependent blocking effects both in human and experimental epilepsy with significant add-on effects to CBZ. Moreover, we show that eslicarbazepine blocks T-type $Ca_v3.2$ channels and exhibits strong antiepileptogenic effects in experimental epilepsy. These results indicate that eslicarbazepine potentially overcomes a cellular resistance mechanism to conventional antiepileptic drugs, and at the same time constitutes a potent antiepileptogenic agent.

Materials and methods

Pilocarpine model of epilepsy

We prepared chronically epileptic rats according to established protocols (Su *et al.*, 2002; Remy *et al.*, 2003*b*). Briefly, male Wistar rats (150–200 g, age 30 ± 2 days) were injected intraperitoneally with the muscarinic agonist pilocarpine (340 mg/kg body weight), which induced status epilepticus in most animals. To reduce peripheral muscarinic effects, methylscopolamine (1 mg/kg) was injected intraperitoneally 30 min before pilocarpine administration. Convulsions were terminated in responsive animals at 40 min after onset of status epilepticus using diazepam (0.1 mg/kg intraperitoneally). Surviving animals were tended, hydrated and fed with glucose solution for the first day until they recovered from the acute insult. Animals were subsequently video monitored. Within 2 to 6 weeks after status epilepticus, most rats developed a chronic epileptic condition. Only animals with video-documented generalized seizures were included within the chronically epileptic group. Rats were used 22 to 65 days after status epilepticus. Sham-control animals were age-matched and treated identically, with pilocarpine being substituted by saline.

The experiments depicted in Supplementary Fig. 4 were carried out in mice. Male CD-1 mice (25–30 g) were purchased from Harlan. Pilocarpine and scopolamine were dissolved in 0.9% NaCl solution. Diazepam was dissolved in 30% dimethyl sulphoxide (DMSO) in 0.9% NaCl with a drop of Tween 80. In mice, the pilocarpine dose was lowered to 300 mg/kg intraperitoneally, otherwise, treatment was identical. Sham animals received 0.9% NaCl solution instead of pilocarpine. Status epilepticus was terminated with 4 mg/kg subcutaneous diazepam 40 min after the onset of status epilepticus. All animal procedures were conducted in strict adherence to the European Directive for Protection of Vertebrate Animals Used for Experimental and Other Scientific Purposes (86/609CEE) and Portuguese legislation (Decreto-Lei 129/92, Portarias

1005/92 e 1131/97). Pilocarpine hydrochloride and (−)-scopolamine hydrobromide trihydrate were supplied by Sigma. Diazepam and ESL were obtained from BIAL - Portela & C[a], S.A.

Eslicarbazepine acetate treatment regimen

For *in vivo* treatment, ESL was dispersed in 0.2% hydroxypropylmethylcellulose (HPMC) in distilled water. Nine days after pilocarpine-induced status epilepticus, pilocarpine-treated mice were randomized and allocated to one of three groups: vehicle 0.2% HPMC ($n = 8$), ESL 150 mg/kg ($n = 6$) or ESL 300 mg/kg ($n = 10$). Sham mice ($n = 10$) received vehicle. Animals were administered per os (p.o.) once-daily for 6 weeks (administration volume = 10 ml/kg).

In vivo EEG recording

In vivo EEG recording was carried out as described by Weiergräber *et al.* (2005). Seven weeks after the end of ESL treatment, mice were anaesthetized (75 mg/kg ketamine and 1 mg/kg medetomidine intraperitoneally) and given 7.5 mg/kg subcutaneous carprofen. A midline 2-cm skin incision on the head and neck was made and the subcutaneous tissue was bluntly separated. A TA11ETA-F10 telemetry device (Data Sciences International) was implanted into a subcutaneous dorsal pocket and leads were coiled into a loop and anchored to surrounding tissue. Two burr holes (0.7 mm in diameter) were positioned with an electric high-speed drill. Electrodes were shortly bent at the tip and placed directly on the dura mater (epidural lead placement) in a bipolar deflection following manufacturer instruction coordinates: (+)-lead: −1 mm/+1 mm to bregma (left hemisphere); (−)-lead: +1 mm/−1 mm caudal of bregma (right hemisphere). Electrodes were secured on the skull with glass ionomer cement. After the cement has dried the scalp was closed. Animals were allowed to recover for 1 week before experiments. EEG continuous recording was performed for 7 days after recovery. Raw data acquisition was performed with Dataquest A.R.T.TM software and analysed with Neuroscore^{TM} software (Data Sciences International). EEG signal was digitized at a sampling rate of 500 Hz/recording-channel. Seizure detection was defined through specific parameters. A dynamic spike detection was used with the minimum value of 100 µV and the maximum ratio of 2 and a threshold ratio of 1.4. The spikes were defined as follows: spike duration from 1 ms to 500 ms, spike interval from 0.005 s to 0.5 s with train duration of at least 5 s. Analyses were validated by off-line visual inspection of the traces. Spikes train duration between 5 and 15 s are characterized in spindle-shaped activity without any phenotypic alteration in video observation. Events that last >15 s are known to correspond to a pathologically epileptiform activity (Bernard *et al.*, 2004; Albayram *et al.*, 2011). EEG recordings were performed 8 weeks after the end of ESL treatment (Fig. 5A).

Rotarod test

Tests were performed 4 weeks after the end of ESL treatment. Motor coordination was evaluated by the Rotarod and wire test. The Rotarod test detects neurological deficit (Dunham and Miya, 1957). Mice were placed on a rotating rod (UGO-Basile, model 7650) at a constant speed of 15 rpm for 3 min. The time that a mouse maintains its balance on the rotating drum was recorded.

Blood sampling and brain collection

In satellite experiments, naive CD1 mice were used for blood sampling and brain collection. For each dose of ESL, four mice were orally dosed and sacrificed 0.5, 1, 2, 4, 8 and 24 h post-dosing by decapitation. The blood was collected into heparinized plastic vials and well shaken before being placed in ice. Samples were then centrifuged at 1500 *g* for 5 min with 200 µl plasma collected from each sample. The plasma and brain samples were placed into plastic vials stored in a freezer (−80°C) until analysis.

Analysis of eslicarbazepine acetate and metabolites

Brain and plasma concentrations of ESL, eslicarbazepine, (R)-licarbazepine and oxcarbazepine (OXC) were determined using a validated enantioselective LC-MS/MS assay, as previously described (Loureiro *et al.*, 2011). Plasma samples (100 µl) were added with 400 µl of internal standard (ISTD) working solution (2000 ng/ml of 10, 11-dihydrocarbamazepine in phosphate buffer pH 5.6) and then processed by solid phase extraction. After thawing and weighing, 0.1 M sodium phosphate buffer (pH 5.6) was added to the brain samples to give a tissue concentration of 0.1 g/ml. The samples were then homogenized using a Heidolph DIAX 900 mixer and transferred to 10 ml plastic centrifugation tubes. After centrifugation at 10 000 *g* for 30 min at 4°C, 0.5 ml of supernatants were added to 0.5 ml ISTD working solution and then processed by solid phase extraction. The samples were placed on an automatic liquid handler (ASPEC-XL4, Gilson) for solid phase extraction using Oasis, HLB, (30 mg, Waters) pre-conditioned with 1 ml of acetonitrile and washed twice with 1 ml of water. Specimens (400 µl) were loaded onto the cartridges and washed twice with 1 ml of water. After the second wash the cartridges were flushed with an air push and then eluted twice with 200 µl of methanol The eluted sample was evaporated until dryness and resuspended into 200 µl of hexane:2-propanol (90:10, v:v). The samples were injected (20 µl) into a LC-MS/MS (Quattro Ultima, Waters) with positive ion detection mode. Separation was performed on a ChiralCel 0.46 cm × 15 cm OD-H column (Chiral technologies). The mobile phase consisted of an isocratic mixture of hexano:ethanol (80:20, v:v; flow rate of 1 ml/min), and ethanol with 5 mM ammonium acetate (added post-column using a flow rate of 0.15 ml/min). A volume of 20 µl was injected and the column temperature kept at 50°C for the run time of 7 min. Electrospray ionization was used for all mass spectrometer methods with a cone voltage of 40 V and capillary current of 3.8 kV. The multiple reaction monitoring pair was m/z 239.1 → 194, collision 40 eV for ISTD; 253.1 → 208, collision 25 eV for OXC; 255.1 → 194, 237, collision 30 eV for eslicarbazepine and (R)-licarbazepine; 297.1 → 194, 237, collision 30 eV for ESL. The autosampler cooler was maintained at 10°C. The samples were quantified with accuracy and precision over the analytical range of 0.2 to 8.0 nmol/ml for plasma and 2.0 nmol/g to 80 nmol/g for brain. The limit of quantification was 0.2 nmol/ml and 2.0 nmol/g, for plasma and brain, respectively.

Estimation of pharmacokinetic parameters

Plasma pharmacokinetic parameters of the parent compound ESL and R-licarbazepine could not be calculated, because ESL was not detected in any samples and R-licarbazepine, when detected, appeared below the limit of quantitation (LOQ) of the assay. The brain and plasma pharmacokinetic parameters of eslicarbazepine and OXC were estimated using non-compartmental analysis (Supplementary Table 1). Eslicarbazepine (S-Lic) was the major metabolite in plasma, evidenced by the $C_{max}plasma_{S\text{-}Lic}/C_{max}plasma_{OXC}$ and $AUC_{0\text{-}t}plasma_{S\text{-}Lic}/AUC_{0\text{-}t}plasma_{OXC}$ ratios far greater than the unit, 10.4 and 4.7 or 16.8 and 6.9 after a single oral dose of 150 or 300 mg/kg ESL, respectively. Thereby, as assessed by using $AUC_{0\text{-}t}$, eslicarbazepine represented 82–87% of total systemic drug exposure, whereas OXC corresponded to ~13–18% after a single oral dose of 150 or 300 mg/kg ESL, respectively.

In agreement with the plasma data, only eslicarbazepine and OXC were found in quantifiable amounts in the brain. As eslicarbazepine and OXC have strong preference to stick to tissue material in a ratio of ~50:1 and such tissue constitutes only 20% of the total brain volume, it is expected that the effective concentrations of eslicarbazepine and OXC in the organic fraction of the brain will be higher than measured in the whole brain volume. Indeed, eslicarbazepine does not show a strong affinity for binding (~30%) to non-specific proteins (Bialer and Soares-da-Silva, 2012) and may preferentially be associated with membranes, which even constitute a smaller fraction (10% to 12%) of the dry weight of the brain (Pratt *et al.*, 1969; Banay-Schwartz *et al.*, 1992). The calculated LogP of eslicarbazepine and OXC are 1.72 and 1.80, according to the software package ADMET Predictor (SimulationsPlus, Inc), which corresponds to an octanol:water partitioning coefficient of 52.5. In the brain, it is also expected that eslicarbazepine and OXC will associate preferentially with organic tissue (lipids and proteins). After 72 h dehydration at 90°C, the water fraction in the mouse brain was found to be ~80% of the brain mass (or volume) and therefore, in an average mouse brain of 358 ± 8 mg ($n = 12$), water comprises 281 ± 6 µl ($n = 12$), while the remaining 80 µl is comprised of cell structures, membranes, lipids, or proteins. Thus, a conservative estimate of the concentration of eslicarbazepine and OXC in the organic fraction of the brain is ~4.6 times higher than that measured directly in the total brain volume (estimated values given in Supplementary Table 1). As assessed by using $AUC_{0\text{-}t}$, eslicarbazepine represented 67–72% of brain (organic phase) drug exposure, whereas OXC corresponded to ~28–33% after a single oral dose of 150 or 300 mg/kg ESL, respectively, which was slightly different from that observed in plasma.

Histology

Hippocampal slices were cut into 20 µm transverse sections using a cryostat (Leica CM3050S, Leica Biosystems) and sections were placed into 0.1 M phosphate buffer and mounted onto glass slides. Sections were stained with Timm stain (Holm and Geneser, 1991). Briefly, for Timm stainings, sections were post-fixed through 95%, 70% and 50% ethanol, rehydrated in distilled water for 20–30 min, then dipped in 0.5% gelatine and allowed to dry overnight. Slides were developed in a solution of 0.11% silver lactate, 0.85% hydroquinone, 30% gum arabic colloid (all w/v) in 0.2 M citrate buffer for 1–1.5 h and then rinsed, counterstained with neutral red, dehydrated, cleared, and coverslipped. Images were collected using Axioskope2 microscope connected to AxioCam camera (Zeiss microscopy). Mossy fibre sprouting was scored using the method of Tauck and Nadler (1985). Briefly, supragranular Timm staining was scored as 0, occasional or no staining; 1, scattered staining in all supragranular regions; 2, patches of heavy staining or continuous light staining; and 3, dense continuous band. Scoring of Timm staining was carried out blinded to the treatment group.

For NeuN staining, 500 µm blocks of brain tissue were immersed in paraformaldehyde for 16 h, then transferred to Dulbecco's phosphate-buffered saline without Ca^{2+} and Mg^{2+} (PBS Dulbecco, Biochrom, Merck Millipore) for 2–3 days. Tissue was then transferred to sucrose solutions of increasing concentration (10, 20 and 30%) over 2 days, before 20-µm thick transverse slices were cut using a microtome (see above). Sections were mounted onto glass slides (Superfrost™ Plus, Thermo Scientific) and left to dry at room temperature. Sections were then immerged into PBS for 10 min, before they were transferred to PBS with 0.3% Triton™ X-100 and 5% normal donkey serum (NDS; Jackson Immuno Research) for 45 min. After a further wash in PBS, sections were incubated 16–24 h at 4°C with the primary antibody (1:1000 anti-NeuN rabbit polyclonal #ABN78, Santa Cruz Biotechnology Inc.; dissolved in PBS and 2% NDS). Next, sections were washed in PBS and exposed to the secondary antibody (1:500 Cy3 donkey anti-rabbit, Dianova; dispensed in PBS and 2% NDS). Sections were examined under a fluorescent microscope (Axio Observer, Zeiss) and pictures taken using ProgRes® camera and ProgRes® Mac Capture Pro 2.7.6. acquisition software (Jenoptik AG). Analysis of cell numbers in CA1, CA3 and DG regions was performed in a semi-automated fashion using a custom MATLAB (Mathworks) routine combined with visual control. The determination of cell numbers was done blinded to the experimental group.

Preparation of hippocampal slices

Rats were deeply anaesthetized (ketamine 100 mg/kg and xylazine 15 mg/kg) and perfused through the heart with ice-cold sucrose-based artificial CSF containing (in mM): NaCl 60, sucrose 100, $NaHCO_3$ 26, KCl 2.5, NaH_2PO_4 1.25, $MgCl_2$ 5, $CaCl_2$ 1, and glucose 20, pH 7.4, adjusted with NaOH, osmolality 305 mOsm. After decapitation, the brain was rapidly removed and transverse slices (300 or 400 µm) were prepared with a vibratome (VT1200S, Leica). The slices were subsequently transferred to a storage chamber filled with carbogenated sucrose artificial CSF (95% O_2, 5% CO_2) and then gradually warmed to 36°C in a water bath and maintained at this temperature for 30 min. Afterwards, the slices were transferred to a second storage chamber filled with artificial CSF containing (in mM): NaCl 125, $NaHCO_3$ 26, KCl 3.5, NaH_2PO_4 1.25, $MgCl_2$ 2, $CaCl_2$ 2, and glucose 15, pH 7.4, adjusted with NaOH, osmolality 305 mOsm, where they were maintained for up to 6 h at room temperature. After an equilibration period of 60 min, they were either used for preparation of acutely dissociated neurons for voltage-clamp recordings (see below) or used for patch-clamp recordings from intact neurons in the slice preparation.

Human specimens from patients with epilepsy

Surgical specimens were obtained from 25 patients with therapy-refractory TLE (Table 1). The histopathology of these specimens showed typical features of Ammon's horn sclerosis in 16 cases, Rasmussen's encephalitis (Patients 15, 20 and 24), moderate mesial temporal damage (Patient 1), tumour (Patient 10), hemimegalencephaly (Patient 23) and cortical dysplasia (Patient 19). Most patients suffered from complex partial and secondary generalized seizures. In addition to these specimens, we obtained one reference specimen (Patient 11). This patient suffered from an angioma and was responsive to CBZ. Human hippocampal slices were prepared as described above for rat slices.

Preparation of dissociated dentate granule cells

For dissociation, 400 µm hippocampal slices were retrieved from the storage chamber one at a time and transferred into 5 ml of saline containing (in mM): methanesulphonic acid Na^+ salt (CH_3SO_3Na) 145, KCl 3, $MgCl_2$ 1, $CaCl_2$ 0.5, HEPES 10, and glucose 15, pH 7.4 adjusted with NaOH, osmolality 308 mOsm. Pronase (Protease type XIV, 2 mg/ml, Fluka, Sigma-Aldrich) was added to the saline and oxygenated with 100% O_2. Enzymatic incubation was carried out for 12 min at 36°C in a water bath, and a subsequent 10 min at room temperature. Slices were then retrieved and washed in pronase-free saline solution of identical composition. The dentate gyrus subfield was dissected and triturated with fire-polished pipettes of decreasing aperture in a Petri dish, which was then mounted onto the stage of an inverted microscope (Axiovert100, Zeiss). We allowed the cells to settle for at least 10 min before starting recordings.

Voltage-clamp recordings in dissociated cells

Properties of I_{NaT} (transient Na^+ current) were examined in dissociated granule cells, which were superfused with an extracellular solution containing (in mM): CH_3SO_3Na 40, tetraethylammonium (TEA) 90, $CaCl_2$ 0.2, $MgCl_2$ 2, HEPES 10, 4-aminopyridine 5, $CdCl_2$ 0.2, and glucose 15, pH 7.4 adjusted with NaOH, osmolality 315 mOsm. Patch pipettes (resistance: 4 ± 1 MΩ) were filled with an intracellular solution containing (in mM): CsF 110, TEA 20, $MgCl_2$ 2, HEPES 10, EGTA 11, ATP-Na_2 5 and GTP-Tris 0.5, pH 7.2 adjusted with CsOH, osmolality 300 mOsm. Properties of I_{NaP} (persistent Na^+ current) in dissociated DG neurons were examined with

Table 1 Patients with refractory TLE (Patients 1–10 and 12–26) and non-refractory TLE (Patient 11)

Patient	Experiment[a]	Age at surgery (years)	Age at onset (years)	Type of seizure	CBZ treatment	Antiepileptic drugs/adjunctive medication	Neuropathology
P1	1	17	13	SGS		LEV, LTG, VPA	Moderate MTD
P2	1	24	12	CPS	+	GBP, LEV, VPA	AHS
P3	1	43	<1	CPS, SGS	+	LCM, LEV, LTG, OXC, PHB, TPM, VGB	AHS
P4	1	55	29	SGS	+	CLB, GBP, LEV, VPA	AHS
P5	1	22	13	SPS, CPS		GBP, LCM, LEV, LTG, VPA	AHS
P6	1	47	15	CPS	+	LEV, LTG, PHB, PHT, TPM, VGB, VPA	AHS
P7	1	57	34	SPS, CPS, SGS	+	OXC	AHS
P8	1	31	3	CPS, SGS	+	LEV, LTG, OXC, PGB, TPM, VPA	Non-lesional TLE
P9	1	22	<1	CPS, SGS	+	LCM, LTG	AHS
P10	1	45	27	SPS, CPS, SGS		LEV, TPM, VPA	Tumor
P11	1	41	41	CPS	+		Angioma
P12	2	31	3	CPS, SGS	+	LTG, VPA, TPM, PGB	AHS
P13	2	28	3	CPS; SGS	+	LEV, VPA, PHT, LTG	AHS
P14	2	24	16	CPS	+	LTG, ESL, VPA, LEV	AHS
P15	2	5	1	CPS, SGS		LEV	RE
P16	2	72	34	SPS	+	LTG, LCM, OXC, ESL, VPA, PHT, TPM, LEV, ZNS, VGB, PHB, PRM	AHS
P17	2	42	<1	SPS, CPS, SGS	+	OXC, VPA, LTG, LCM, TPM, LEV, TGB, VGB, ETS, MSM, STR	AHS
P18	2	37	33	CPS, SGS	+	LTG, LEV	AHS
P19	2	<1	<1	CPS	+	OXC, LEV, TPM	Cortical dysplasia
P20	3	16	11	SPS, CPS, SGS	+	LEV, ZNS, OXC, ESL	RE
P21	3	29	15	CPS	+	LEV, LCM	AHS
P22	3	26	19	CPC		LTG, LCM, OXC, VPA, TPM, LEV	AHS
P23	3	4	<1	SPS, CPS	+	VPA, LEV, PHT, CLB, TPM, PHB, CZP	Hemimegalencephaly
P24	3	10	5	CPC, SGS		LEV, ETS, VPA, OXC, LTG, STM, RUF	RE
P25	3	17	<1	SPS, CPS		VPA, LTG, STM	Porencephaly
P26	1	26	13	SPS, CPS, SGS	+	PHT, PHB, LCM, LEV, LTG, TPM, VPA, STM, OXC, VGB	AHS

[a] 1 = I_{NaT}; 2 = I_{NaP}; 3 = Firing.

AHS = Ammon's horn sclerosis; CZP = clonazepam; CLB = clobazam; CPS = complex partial seizures; ETS = ethosuximide; GBP = gabapentin; LCM = lacosamide; LEV = levetiracetam; LTG = lamotrigine; MSM = methosuximide; MTD = mesial temporal damage; PGB = pregabalin; PHB = Phenobarbital; PHT = phenytoin; PRM = primidone; RE = Rasmussen's encephalitis; RUF = rufinamide; SGS = secondary generalized seizures; SPS = simple partial seizures; STR = stiripentol; STM = sulthiame; TGB = tiagabine; TPM = topiramate; VGB = vigabatrin; VPA = valproic acid; ZNS = zonisamide.

an extracellular solution containing (in mM): CH_3SO_3Na 100, TEA 40, $CaCl_2$ 2, $MgCl_2$ 3, HEPES 10, 4-aminopyridine 5, $CdCl_2$ 0.2, and glucose 25, pH 7.4 adjusted with NaOH, osmolality 315 mOsm. The intracellular solution consisted of (in mM): CsF 110, $MgCl_2$ 2, HEPES 10, EGTA 11, ATP- Na_2 2, and GTP-Tris 0.5, pH 7.2 adjusted with CsOH, osmolality 300 mOsm. A liquid junction potential of −10 mV was calculated between the intracellular and extracellular solutions for both set of experiments and corrected. Thus, data points were shifted in a depolarizing direction relative to the voltage axis.

We used an EPC9 amplifier (HEKA) to obtain tight-seal (>1 GΩ) whole-cell recordings. For I_{NaT} recordings, series resistance was ~10 MΩ and could be compensated between 50 and 60%. Even though these recordings were carried out with a reduced Na^+ gradient, Na^+ currents were frequently >5 nA, resulting in unacceptable voltage errors >20 mV. Therefore we partially blocked Na^+ currents with 10 nM tetrodotoxin (Tocris bioscience) added to the bath solution. Measurements where the maximal residual voltage error still exceeded 5 mV were rejected. Currents were filtered at 10 kHz (low-pass Bessel filter), sampled at 50 kHz and recorded by a personal computer using the Patchmaster acquisition software (HEKA). Residual capacitance transients and leak conductance were subtracted with a P/4 protocol. For I_{NaP} recordings series resistance was compensated between 55 and 75%, current signals were filtered at 10 kHz (low-pass Bessel filter) and sampled at 20 kHz. For these recordings we used the Pulse 8.8 acquisition software (HEKA). No P/4 protocol was applied for I_{NaP} recordings. After wash-out of drugs we applied 0.5 µM tetrodotoxin. The resulting current trace was subtracted from all other traces to isolate I_{NaP}.

Time-dependent changes in the voltage-dependence of I_{NaP} have been described. To dissect such changes from pharmacological effects, we carried out I_{NaP} recordings in sham-control animals, identical in method to previous experiments, but without drug application. Indeed, these experiments confirmed the presence of a time dependent shift of -3.08 ± 0.93 mV ($n = 4$, four animals). All experiments in rats were corrected for this shift. In experiments with human tissue voltage of half maximal activation of I_{NaP} under initial artificial CSF perfusion and I_{NaP} after wash out of drugs were interpolated and used as the baseline to take time-dependent changes into consideration.

All voltage-clamp experiments were performed at room temperature (22 ± 1°C). Drugs were applied by hydrostatic pressure via a nearby (50–100 µm) superfusion pipette. At least 2 min were allowed for full exchange of solutions around the recorded cell.

Voltage-clamp recordings in HEK and CHO cells

HEK 293 cells obtained from the European Collection of Animal Cell Culture Cells were maintained in a humidified atmosphere (95% relative humidity) with 5% CO_2 and were grown in Dulbecco's modified Eagle medium/F-12 (with GlutaMAX® I, Gibco BRL) supplemented with 9% foetal bovine serum (GibcoBRL), 0.9% penicillin/streptomycin solution (Gibco BRL) and 100 µg/ml geneticin. Cells were stably transfected with the $hCa_v3.2$ cDNA. Patch-clamp recordings were carried out with a bath solution of the following composition: NaCl 137 mM, KCl 4 mM, CaCl2 1.8 mM, $MgCl_2$ 10 mM, D-glucose 10 mM, HEPES 10 mM, pH 7.4. The intracellular solution consisted of TEACl 137 mM, CsCl 80 mM, Mg-ATP 5 mM, $MgCl_2$ 4 mM, Na_2-GTP 1 mM, phosphocreatine-Tris 20 mM, HEPES 10 mM, EGTA 10 mM, pH (titrated with KOH) 7.2.

Voltage-clamp paradigms and data analysis

To determine the voltage-dependence of activation and inactivation, standard protocols were used. Current values were converted to the conductance G(V) according to $G(V) = I(V) / (V - V_{Na})$, where V_{Na} is the Na^+ reversal potential, V the command potential and I(V) the peak Na^+ current amplitude. G(V) was then fitted for each set of traces obtained from individual neurons with a Boltzmann equation:

$$G(V) = A_1 + \left[(A_0 - A_1)/\left(1 + e^{(V-V1/2)/k}\right)\right],$$

where A_0 and A_1 are Na^+ conductance, $V_{1/2}$ is the voltage at which G(V) is half-maximal conductance, and k represents a slope factor.

Recovery from inactivation was studied with a double pulse protocol (Fig. 1A) with interpulse intervals (Δt) varying from 1 to 8192 ms. An interval of 5 s at −80 mV was interspersed between double pulse protocols to ensure full recovery from inactivation. The time course of recovery was fit with a biexponential equation of the form:

$$I(t) = A_0 + A_{fast}\left(e^{-\Delta t/\tau\,fast}\right) + A_{slow}\left(e^{-\Delta t/\tau\,slow}\right)$$

with τ_{fast} and τ_{slow} representing the fast and slow time constants of recovery, and A_{fast} and A_{slow} the corresponding relative amplitude contributions. Fitting was done using a Levenberg-Marquardt algorithm. In all cases, fits were performed on the data points obtained from individual cells, and the parameters then averaged. All results are presented as the mean ± standard error of the mean (SEM).

For determination of the concentration of drug at half maximal inhibition (IC_{50}), we fit the data with the following equation that incorporates the possibility for incomplete block, i.e. with part of the current resistant to block:

$$current_{peak,relative} = \left(y_1 + \frac{(100 - y_1)}{1 + 10^{([LogIC_{50(1)} - X]H_1)}}\right) + \left(y_2 + \frac{(y_1 - y_2)}{1 + 10^{([LogIC_{50(2)} - X]H_2)}}\right) - y_1$$

where $_1$ denotes parameters for high affinity binding and $_2$ those for low affinity binding. x is the compound concentration, y_1/ y_2 is the remaining peak current amplitude, with y_1 as the maximum current amplitude for the second fit. $IC_{50(1)}$/ $IC_{50(2)}$ is the concentration of drug at half maximal inhibition and H_1/ H_2 is the Hill coefficient for the fit. We fitted with both the two-site model described above, and a single-site binding model with an otherwise equivalent equation. Under these conditions, an F-test revealed that the two-site model is preferred [$F(2,53) = 15.17$, $P < 0.0001$].

Current-clamp recordings

For whole-cell current clamp recordings, 300-µm thick hippocampal slices were placed in a submerged chamber on the headstage of an upright microscope (Axioskop FSI, Zeiss) and perfused (60 ml/min) with carbogenated artificial CSF containing (in mM): NaCl 125, $NaHCO_3$ 26, KCl 3.5, NaH_2PO_4 1.25, $MgCl_2$ 2, $CaCl_2$ 2, and glucose 15, pH 7.4, adjusted with

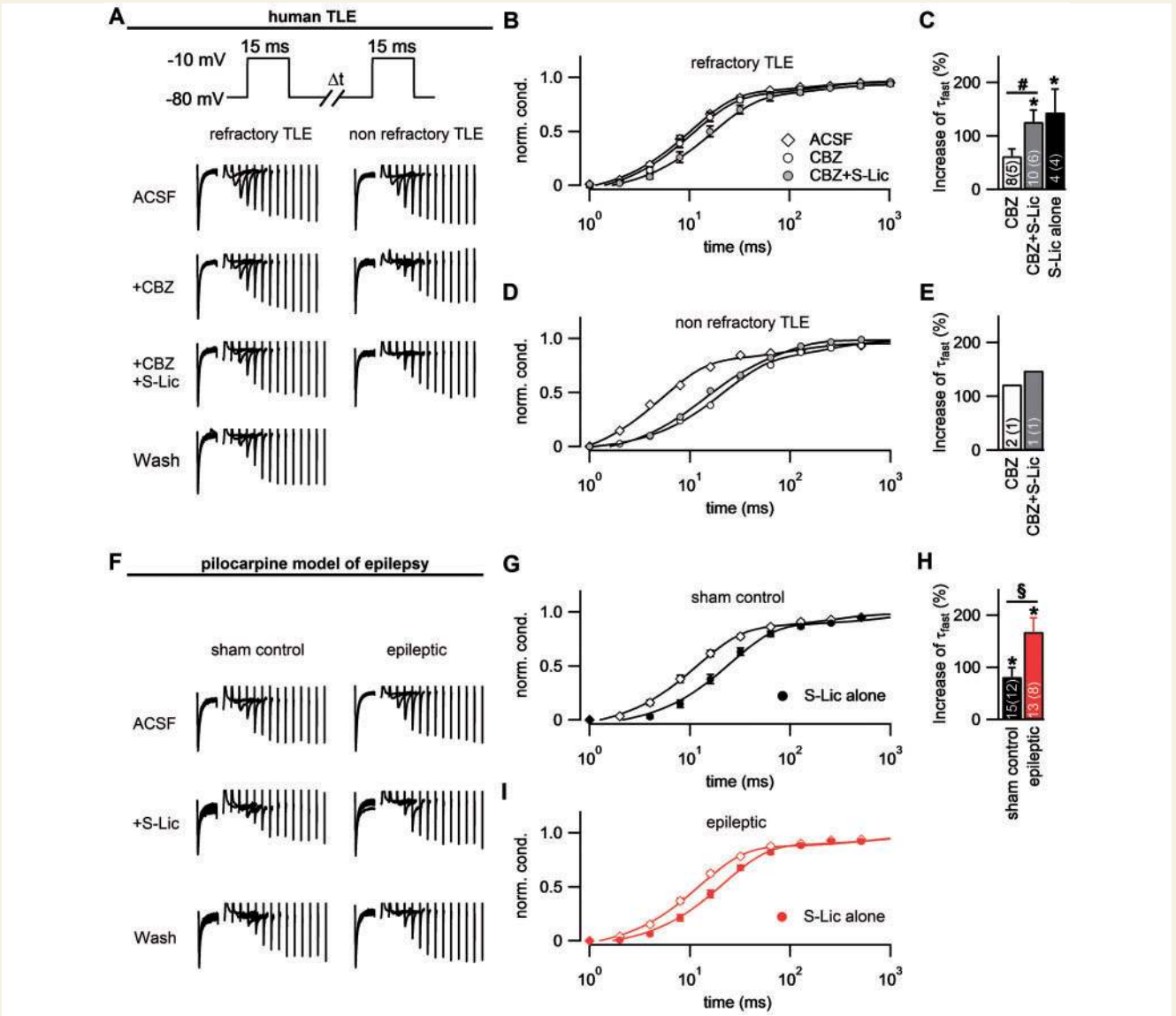

Figure 1 Eslicarbazepine (S-Lic) exhibits maintained activity both in human and experimental TLE. (**A**) Representative experiments showing the effects of 100 μM CBZ and subsequent additional application of 300 μM eslicarbazepine on recovery from fast Na^+ channel inactivation in granule cells from a patient with therapy-refractory TLE and a patient with non-refractory TLE. (**B**–**E**) Time course of recovery from inactivation in granule cells from patients with refractory TLE (**B**) and the patient with non-refractory TLE (**D**). The evaluation of the fast recovery time constant t_{fast} shows a significantly larger increase when eslicarbazepine is applied in addition to CBZ (**C**). In two cells from the non-refractory patient, the effects of CBZ seemed greater and eslicarbazepine did not produce an additional effect (**E**). (**F**–**H**) Effects of eslicarbazepine on fast sodium channel recovery from inactivation in the pilocarpine model of epilepsy. Representative example of 300 μM eslicarbazepine effects on recovery from inactivation in sham-control and epileptic animals (**F**). Recovery from inactivation was slowed in the presence of 300 μM eslicarbazepine in both sham-control (**G**) and epileptic animals (**I**), quantification in panel (**H**). *n*-numbers for cells and animals shown as inset in bars. $^{\#}P < 0.05$ Mann-Whitney U-test; $^{*}P < 0.05$, paired *t*-test; $^{\S}P < 0.05$, Mann-Whitney U-test. S-Lic = eslicarbazepine; ACSF = artificial CSF.

NaOH, osmolality 305 mOsm, temperature 35 ± 1°C. Granule cells were visually identified under difference-interference contrast optics, and patch-clamp recordings were obtained using pipettes with a resistance of 4 ± 1 MΩ. Pipettes were filled with an intracellular solution containing (in mM): Potassium gluconate 130, KCl 5, HEPES-acid 10, EGTA 0.16, Mg-ATP 2, Na_2-ATP 2, pH 7.25 adjusted with KOH, osmolality 295. We calculated and corrected a liquid junction potential of + 15.6 mV between the intra- and extracellular solution. Current-clamp recordings were obtained using an amplifier with an active bridge circuit (Dagan, BVC-700 A). Bridge balance was carefully adjusted before each measurement. The signals were filtered on-line at 5 kHz, digitized at a sampling rate of 100 kHz (Digidata 1320, Molecular Devices) and acquired and stored on hard disk (pClamp 9.2, Molecular Devices). Neurons were uniformly maintained at −80 mV resting potential by small

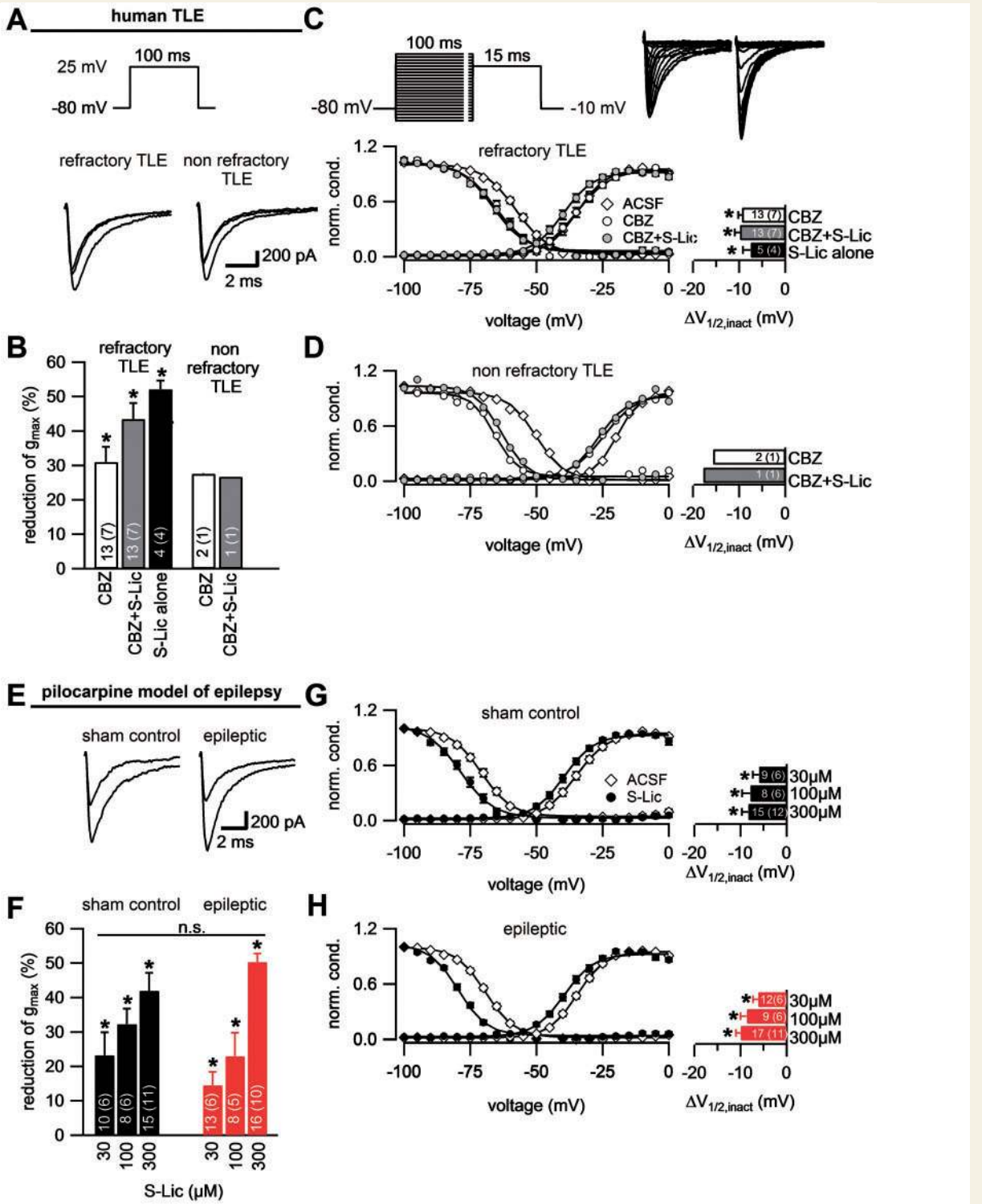

Figure 2 Eslicarbazepine (S-Lic) and CBZ effects on voltage-dependence of voltage-gated sodium channels in human epilepsy (A–D) and experimental epilepsy (E–H). (**A**) In human therapy-refractory TLE and the patient with non-refractory TLE, 100 μM CBZ and additional application of 300 μM eslicarbazepine reduced the maximal conductance of Na^+ channels similarly, as shown in representative neurons. (**B**) Quantification of the reduction of maximal conductance by 100 μM CBZ, 100 μM CBZ plus 300 μM eslicarbazepine and 300 μM eslicarbazepine alone. The effects observed with CBZ could not be further increased by co-applying 300 μM eslicarbazepine. (**C**) Effects on voltage-dependent activation and inactivation. Voltage paradigm and representative examples of a current family shown in *inset*. Horizontal bar graphs show the effects on the voltage of half-maximal inactivation. CBZ caused a significant shift of the voltage-dependence of inactivation into a hyperpolarizing direction in human specimens. Additional application of 300 μM eslicarbazepine did not have any significant further effects. (**D**) Effects of 100 μM CBZ and CBZ plus 300 μM eslicarbazepine in the non-refractory patient. Similar results as for the refractory patients in **C** were obtained. (**E** and **F**) Dose-dependent effects of eslicarbazepine on maximal sodium channel conductance in experimental epilepsy.

(continued)

current injections (maximal current injection magnitude −200 pA) to ensure uniform conditions for examination of action potential properties. Action potential morphology was characterized using short current injections (3 ms), and repetitive firing was elicited by prolonged (500 ms) current injections. Igor Pro 9.12 (Wavemetrics) was used to extract quantitative parameters describing properties of action potentials (peak amplitude, maximal rate of rise of the voltage trace, and the half-width measured at the voltage intermediate between action potential threshold and peak). The action potential threshold was defined as the voltage at which the slope of the voltage trace was >15 mV/ms (Sekerli *et al.*, 2004). Passive membrane properties were examined using small subthreshold current injections.

Drugs

CBZ (Sigma) and eslicarbazepine (BIAL - Portela & C[a]) were dissolved in DMSO. In all pharmacological experiments, control artificial CSF contained equal amounts of DMSO (0.1%). For experiments on $I_{NaP,}$ CBZ was dissolved in ethanol, of which identical concentrations were used in all control and CBZ-containing solutions. All chemicals for solutions were acquired from Sigma-Aldrich, unless stated otherwise.

Statistical analysis

For statistical comparison the Student's *t*-test was used as appropriate with a significance level α set at 0.05. When comparing the recordings before and during application of drugs, paired tests were used, when performing group comparisons of control and epileptic group, unpaired tests were used. Significance levels of <0.05 are marked with asterisks in figures. Statistical tests were used as indicated. Data fitting a normal parametric distribution were analysed using ANOVA followed by appropriate *post hoc* tests (Dunnett's or Newman-Keuls post-test. Where appropriate, non-parametric Mann-Whitney U or Kruskal-Wallis tests were used. Results are presented as mean ± SEM.

Results

Use-dependent blocking effects of most sodium channel blocking anticonvulsants hinge upon a pronounced slowing of the recovery from fast Na^+ channel inactivation. In human hippocampal neurons from patients with therapy-refractory epilepsy (see Table 1 for clinical data) we found that the recovery from inactivation was not affected by high concentrations of 100 µM CBZ (Fig. 1A–C), as also shown previously (Remy *et al.*, 2003*a*). Next, we tested if adding eslicarbazepine has additional effects. At concentrations of eslicarbazepine at which the effects on recovery from inactivation saturate (300 µM, Supplementary Fig. 1A), adding eslicarbazepine potently slowed the recovery from inactivation (Fig. 1B and C). Application of eslicarbazepine alone also significantly slowed the recovery from inactivation (Fig. 1C). In a single patient clinically responsive to CBZ (Patient 11 in Supplementary Table 1), CBZ strongly slowed recovery from inactivation without eslicarbazepine having additional effects (Fig. 1A, D and E). These results suggest that eslicarbazepine has a significant add-on effect compared to CBZ alone in human epilepsy patients. However, a comparison to control tissue cannot be extensive in human tissue and completely normal tissue is not available.

In animal models of epilepsy, however, the efficacy of eslicarbazepine in inhibition of Na^+ channels can be rigorously compared between chronically epileptic and control animals. Indeed, in the pilocarpine model of epilepsy, Na^+ channel recovery from inactivation becomes insensitive to CBZ (Remy *et al.*, 2003*b*). We therefore set out to examine if this is also the case for eslicarbazepine or if eslicarbazepine retains efficacy in chronically epileptic animals. We found that eslicarbazepine significantly slowed the time course of recovery in both sham-control animals (Fig. 1F and G) as well as in pilocarpine-treated animals (Fig. 1F and I, summary in Fig. 1H and Supplementary Fig. 1B). At the highest concentration of eslicarbazepine tested (300 µM), the effects were even larger in epileptic animals (Fig. 1H). These results indicate that eslicarbazepine activity is maintained both in human and experimental epilepsy.

This effect was selective to recovery from inactivation. In human specimens, eslicarbazepine did not show add-on effects to CBZ on other properties of transient Na^+ currents (I_{NaT}). In both human therapy-refractory TLE and the patient with non-refractory TLE, the effects observed on maximal sodium channel conductance with CBZ could not be further increased by co-applying 300 µM eslicarbazepine (Fig. 2A and B). We also examined effects on voltage-dependent activation and inactivation. Expectedly, CBZ caused a significant shift of the voltage-dependence of inactivation to a hyperpolarizing direction in human specimens, with no further effects by additional application of 300 µM eslicarbazepine (Fig. 2C and D).

In the pilocarpine model of epilepsy, significant effects of eslicarbazepine were observed on the maximal sodium channel conductance (asterisks indicate $P < 0.05$, paired *t*-test). These were not significantly different in control

Figure 2 Continued

Representative traces in **E** with application of 300 µM eslicarbazepine. Between control and epileptic animals, no differences in eslicarbazepine effects on the maximal conductance could be observed at any concentration tested. (**G** and **H**) Effects of 300 µM eslicarbazepine on voltage-dependent activation and inactivation. Horizontal bar graphs show changes in the voltage of half-maximal inactivation with increasing doses of eslicarbazepine as indicated. The effects of eslicarbazepine on the voltage-dependence of inactivation were not different in epileptic compared to control animals at any concentration of eslicarbazepine. *n*-numbers for all experiments given within the bars with number of patients/animals in brackets. *$P < 0.05$ paired *t*-test. S-Lic = eslicarbazepine.

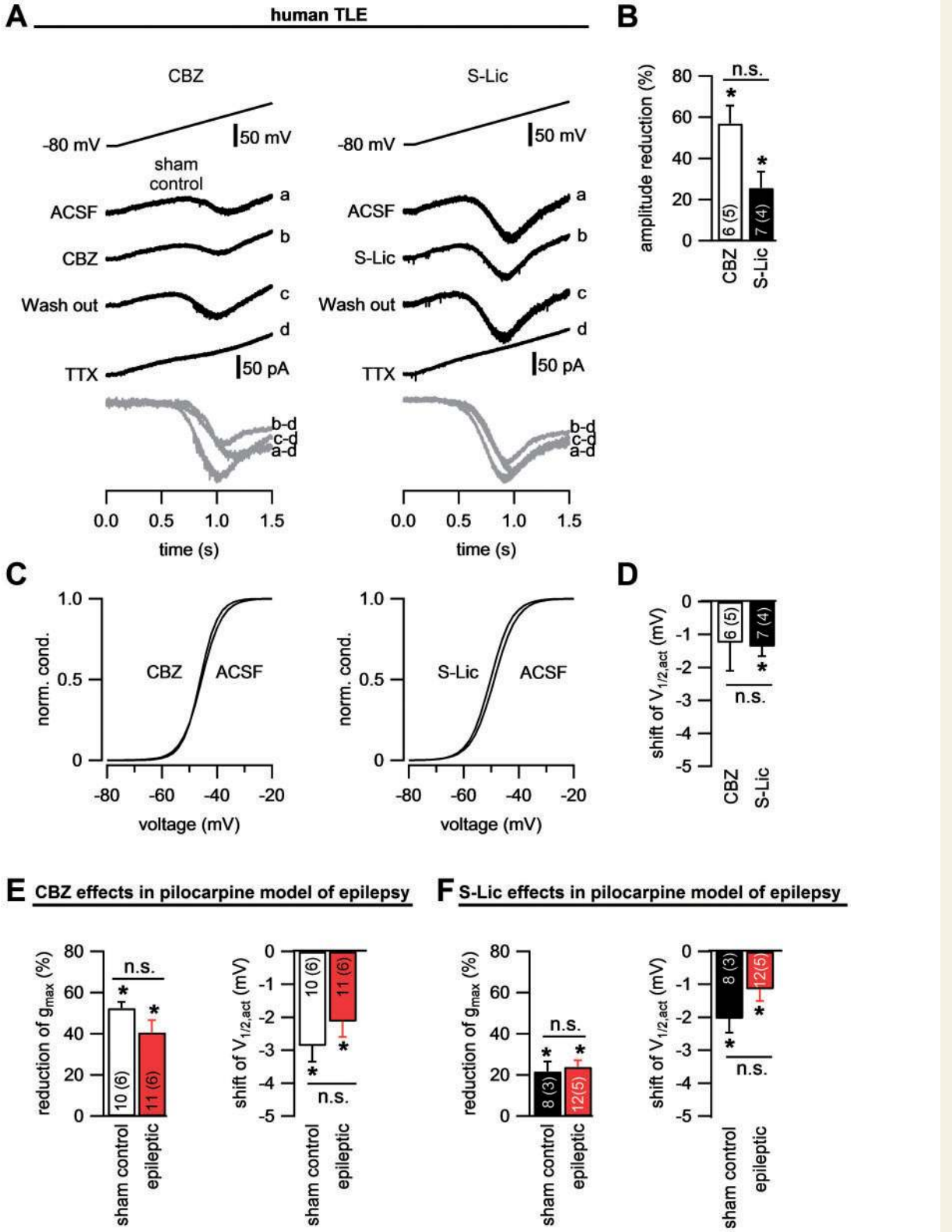

Figure 3 Effects of CBZ and eslicarbazepine (S-Lic) on persistent Na^+ currents (I_{NaP}) in human and experimental epilepsy. (**A**) I_{NaP} was elicited by slow voltage ramps (50 mV/s, *top*) in isolated human granule cells. Representative current traces before (trace a), during (trace b) and after washout (trace c) of 100 μM CBZ or 300 μM eslicarbazepine, and subsequent tetrodotoxin application (trace d) are depicted. *Bottom* traces show isolated I_{NaP} after subtracting currents obtained under tetrodotoxin application from all other traces. (**B**) Average reduction of maximal conductance. Both CBZ and eslicarbazepine decreased the magnitude of I_{NaP}. (**C**) Current traces were fitted with a Boltzmann equation corrected for the driving force. The voltage dependence of conductance was reconstructed from the averaged parameters derived from all analysed human granule cells, normalized to the maximal conductance and plotted versus the voltage. (**D**) The voltage dependence showed only

(continued)

compared to epileptic rats at any concentration tested (Fig. 2E and F). Likewise, the effects of 300 μM eslicarbazepine on voltage-dependent activation and inactivation (Fig. 2G and H) proved to be indistinguishable between control and epileptic rats.

In addition to I_{NaT}, most neurons exhibit a persistent Na^+ current component (I_{NaP}; Magistretti and Alonso, 1999; Uebachs *et al.*, 2010; Doeser *et al.*, 2014). We elicited I_{NaP} using slow voltage ramps (50 mV/s) in isolated human granule cells. A sequential application of either 100 μM CBZ or 300 μM eslicarbazepine, followed by complete block of sodium channels with tetrodotoxin allowed us to isolate I_{NaP} by subtraction (Fig. 3A). CBZ and eslicarbazepine caused a significant reduction in the I_{NaP} magnitude (Fig. 3B). Effects on the voltage dependence of I_{NaP} activation were very small (in the order of 1 mV; Fig. 3C and D) and showed only minor changes.

Chronic experimental epilepsy does not seem to affect the sensitivity of I_{NaP} to CBZ and eslicarbazepine (100 and 300 μM). Both anticonvulsants reduce the I_{NaP} conductance significantly in both sham-control and pilocarpine-treated rats, with no differences between groups. Likewise, effects on the voltage-dependence of activation were unaltered when comparing sham-control and pilocarpine-treated animals (Fig. 3E and F).

The selective loss of CBZ efficacy on I_{NaT} raises the question if eslicarbazepine is more effective than CBZ in modulating neuronal repetitive firing in chronic epilepsy. We obtained whole-cell patch-clamp recordings from human dentate gyrus cells in the slice preparation, and examined their firing behaviour during prolonged (0.5 s) current injections (Fig. 4A). In these experiments, we used CBZ concentrations close to the maximal brain tissue concentration (30 μM; Rambeck *et al.*, 2006), which significantly reduced the maximal firing frequency (Fig. 4A and B). However, when we subsequently co-applied 100 μM eslicarbazepine, a significant additional effect was observed (Fig. 4B). Eslicarbazepine alone was also capable of reducing maximal firing rates (100 μM eslicarbazepine, Fig. 4B; for dose-response relationship for eslicarbazepine see Supplementary Fig. 2A). We then analysed how the effect of CBZ on firing behaviour develops during prolonged current injections. A clear use-dependence was observed, with increased efficacy for longer current injection durations (Fig. 4C and D). Additional application of eslicarbazepine produced additional block at the longest time point of 500 ms (Fig. 4C and D).

In experimental epilepsy, eslicarbazepine was equally effective in inhibiting firing of dentate gyrus cells in control versus pilocarpine-treated rats (Fig. 4E and H), independent of the applied dose (Supplementary Fig. 2B). This was apparent when analysing the development of blocking effects with increasing current injection durations (Fig. 4E). In marked contrast, the use-dependent effects of CBZ on neuronal firing were significantly reduced in chronic experimental epilepsy (Fig. 4F). In this model, we also applied both CBZ and eslicarbazepine concurrently. This resulted in a blocking activity that was similar to eslicarbazepine alone (Fig. 4G). When the reduction of maximal firing rates was quantified, the following conclusions could be made. Firstly, all drugs or drug combinations significantly inhibited firing (Fig. 4H). Secondly, the effects of CBZ were considerably reduced in chronic epilepsy, whereas those of eslicarbazepine were not (Fig. 4H). Finally, in contrast to the human situation, the application of both CBZ and eslicarbazepine did not cause larger blocking effects either in sham-control or in epileptic animals compared to CBZ alone. Nevertheless, the results so far suggest that eslicarbazepine shows a maintained activity in human tissue in which resistance to CBZ is observed. In addition to a maintained anticonvulsant activity, it would also be desirable to achieve an antiepileptogenic activity, defined as the capability to affect the transition of a normal to an epileptic brain. We were motivated to examine this question because we discovered that eslicarbazepine is capable of potently inhibiting neuronal T-type Ca^{2+} channels, in particular $Ca_v3.2$. This channel has been shown to play a crucial role in epileptogenesis, with genetic deletion resulting in strongly reduced spontaneous seizure frequency and neuronal damage in the pilocarpine model of epilepsy (Becker *et al.*, 2008). We used whole-cell patch-clamp recording to examine the effects of eslicarbazepine on $hCa_v3.2$ calcium channels stably expressed in HEK 293 cells. Depolarization from −80 to −25 mV evoked large T-type Ca^{2+} currents, that were strongly blocked by low concentrations of eslicarbazepine ranging from 0–30 μM (Fig. 5A). Additional block was observed at higher concentrations up to 1000 μM (Fig. 5A). As expected, $Ca_v3.2$ channels were sensitive to mibefradil, but displayed a low sensitivity to valproate (Fig. 5B). In contrast to T-type channels, the high-

Figure 3 Continued

minor changes. From **A–D**, it is clear that both CBZ and eslicarbazepine decrease the magnitude of the persistent Na^+ current, with only small changes in the voltage dependence of activation. (**E**) In chronic experimental epilepsy, CBZ and eslicarbazepine reduced the I_{NaP} conductance significantly in both sham-control and pilocarpine-treated rats. (**F**) The I_{NaP} voltage-dependence of activation was shifted into a hyperpolarizing direction following CBZ application for sham control and pilocarpine treated rats. A similar hyperpolarizing shift was observed for eslicarbazepine in both groups. The effects of neither CBZ nor eslicarbazepine on I_{NaP} were altered when comparing sham-control and pilocarpine-treated animals (indicated with n.s.). *n*-numbers for all experiments given within the bars with number of patients/ animals in brackets. $^*P < 0.05$. S-Lic = eslicarbazepine; TTX = tetrodotoxin; ACSF = artificial CSF.

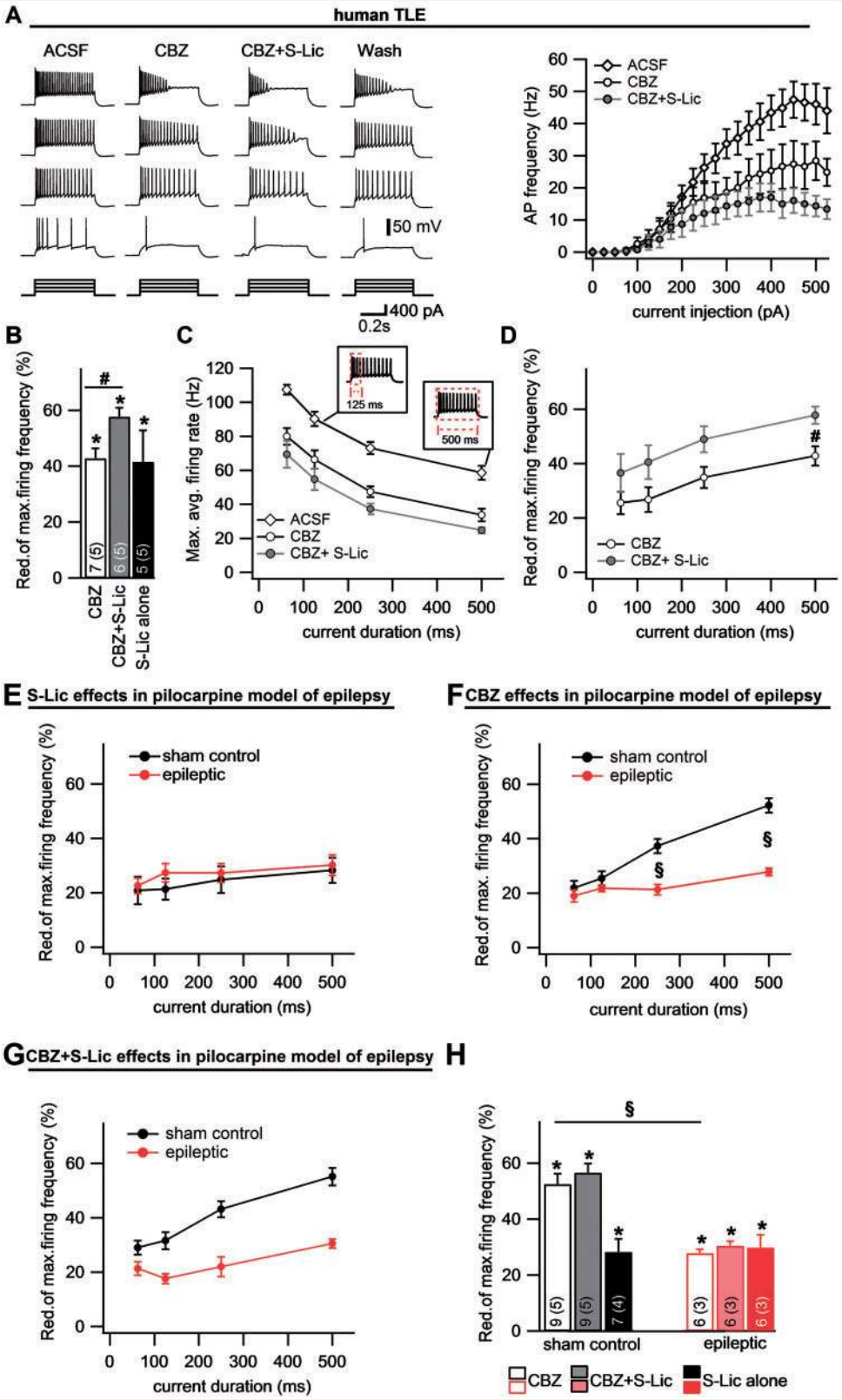

Figure 4 Effects of CBZ and eslicarbazepine (S-Lic) on neuronal firing behaviour. (**A**) Whole-cell patch-clamp recordings in current-clamp mode from human dentate gyrus cells from patients with therapy-refractory TLE in the slice preparation. Representative experiment with application of 30 μM CBZ and subsequent co-application of 100 μM eslicarbazepine showing an add-on effect of eslicarbazepine. Mean input-output relations shown in the *right* panel. (**B**) Analysis of maximal firing frequency for all experiments as in **A**, confirming a significant additional effect of eslicarbazepine. (**C** and **D**) Quantification of the development of drug effects during increasing durations of depolarization as the absolute firing frequency (**C**) and the reduction of firing rate in per cent (**D**). (**E** and **F**) Effects of 100 μM eslicarbazepine (**E**) and 30 μM CBZ (**F**) in chronic

(continued)

threshold Ca^{2+} channel $Ca_v2.1$ showed a low sensitivity to eslicarbazepine (measurements in CHO cells, see 'Materials and methods' section; Fig. 5C and E). The dose-response relationship for $Ca_v3.2$ block by eslicarbazepine showed that a block of high affinity occurs with an IC_{50} of 0.43 μM, and a further block at higher concentrations with an IC_{50} of 62.6 μM (Fig. 5D). We fitted data with both a two-site and a single-site binding model (see 'Materials and methods' section). An *F*-test revealed the two-site model to be preferred [$F(2,53) = 15.17$, $P < 0.0001$]. Untransfected control cells were devoid of any T-like current.

Because these results indicated a potent block of $Ca_v3.2$ channels by eslicarbazepine, we examined if this could be exploited as an antiepileptogenic strategy. We induced status epilepticus in mice with pilocarpine. After 9 days of recovery, pilocarpine-treated mice were randomized, allocated to one of three groups and treated for 6 weeks with either vehicle ($n = 8$), 150 or 300 mg/kg ESL ($n = 6$ and 10, respectively; Fig. 6A). Plasma and brain levels of the ESL metabolites were determined after a single oral dose of 150 or 300 mg/kg ESL (Supplementary Fig. 3). These experiments showed that eslicarbazepine was the major metabolite in plasma (Supplementary Fig. 3A and B) and brain (Supplementary Fig. 3C–F). Moreover, an estimate of the concentration of eslicarbazepine in the organic fraction of brain tissue yielded peak values comparable with those used in the *in vitro* experiments in this study (Supplementary Table 1). The corresponding mouse plasma levels are within the range of those observed in patients with partial-onset seizures (Perucca *et al.*, 2011) or healthy volunteers taking ESL at therapeutic doses (Elger *et al.*, 2013).

Mice, as humans, convert ESL to eslicarbazepine, whereas rats convert ESL to OXC. We therefore confirmed in *in vitro* experiments that eslicarbazepine also shows maintained activity on Na^+ channels in epileptic mice (Supplementary Fig. 4).

Eight weeks after the end of treatment, continuous cortical EEG monitoring was carried out for 7 days in all animals. Pilocarpine-treated mice that had received vehicle developed spontaneous electrographic seizures (Fig. 6B, 1.16 ± 0.23/day) whereas sham-control mice never showed seizure activity. In epileptic animals, ANOVA revealed a significant effect of ESL treatment [$F(2,19) = 7.13$, $P = 0.005$]. *Post hoc* tests revealed that both doses of ESL significantly decreased electrographic seizure occurrence to 0.12 ± 0.03/day and 0.39 ± 0.11/day ($P = 0.004$ and 0.021 for 150 and 300 mg/kg ESL, respectively, Dunnett's *post hoc* test, Fig. 6C and D). There was no significant effect of ESL treatment on seizure duration [$F(2,89) = 1.26$, $P = 0.29$], seizures with a duration of >15 s were exclusively observed in vehicle-treated epileptic animals (Fig. 6E).

The Rotarod test revealed severe impairment in motor coordination in epileptic compared to sham-control animals ($P = 0.004$, Mann-Whitney U test). There was no significant effect of ESL treatment over all groups ($P = 0.065$, $\chi^2 = 5.47$) (Fig. 6F). This may be due to the fact that ESL had adverse effects on movement at higher concentrations, as shown by experiments in control animals. Indeed, the median toxic dose (TD_{50}) for motor impairment at the Rotarod test was 313.7 mg/kg body weight, with no significant motor impairment seen at a dose of 150 mg/kg body weight (Supplementary Table 2). These data indicate that transitory treatment with ESL diminishes the development of chronic seizures.

We also found that this treatment reduces the characteristic pattern of neuronal damage and reorganization in epileptic animals. Aberrant mossy fibre sprouting into the inner molecular layer of the dentate gyrus observed in epileptic animals treated with vehicle ($n = 5$, Fig. 6G) was significantly decreased in ESL-treated epileptic mice (Fig. 6G and H, $P = 0.036$, Kruskal-Wallis test, Mann-Whitney post test with Bonferroni correction, effect of 150 mg/kg ESL not significant, 300 mg/kg ESL $P = 0.018$).

Epileptic animals treated with vehicle displayed neuronal loss in the CA1 subfield with sparing of the dentate gyrus (Fig. 6I and J), which was reduced in animals treated with 150 mg/kg ESL, but not those that received 300 mg/kg ESL. ANOVA revealed a significant effect of treatment [$F(3,20) = 6.429$, $P = 0.0032$]. Both the reduction of neuronal density in epileptic vehicle-treated animals compared to sham-control animals, and the attenuation of neuronal cell loss in animals treated with 150 mg/kg ESL were significant (Newman-Keuls post-test, $P < 0.01$ and 0.05, respectively). In the CA3 region, a significant effect of treatment could also be observed [$F(3,21) = 3.346$, $P = 0.039$]. No significant differences in neuronal density were observed in the dentate gyrus (Fig. 6J).

Discussion

There is an urgent need both for novel anticonvulsant and antiepileptogenic therapies. Here, we show that eslicarbazepine overcomes cellular mechanisms of

Figure 4 Continued

experimental epilepsy. Panels represent an analysis of development of block over the duration of the depolarization. In contrast to the human situation, the application of both CBZ and eslicarbazepine did not cause larger blocking effects either in sham-control or in epileptic animals compared to CBZ alone (**G**). (**H**) Quantification of effects of 30 μM CBZ alone, 30 μM CBZ + 100 μM eslicarbazepine and 100 μM eslicarbazepine alone without previous CBZ application. $^{\S}P < 0.05$. *n*-numbers for cells and animals shown in bars. $^{*}P < 0.05$ paired *t*-test; $^{\#}P < 0.05$ Mann-Whitney U test; In **H**, $^{\S}P = 0.0004$, Mann-Whitney U test. S-Lic = eslicarbazepine; ACSF = artificial CSF.

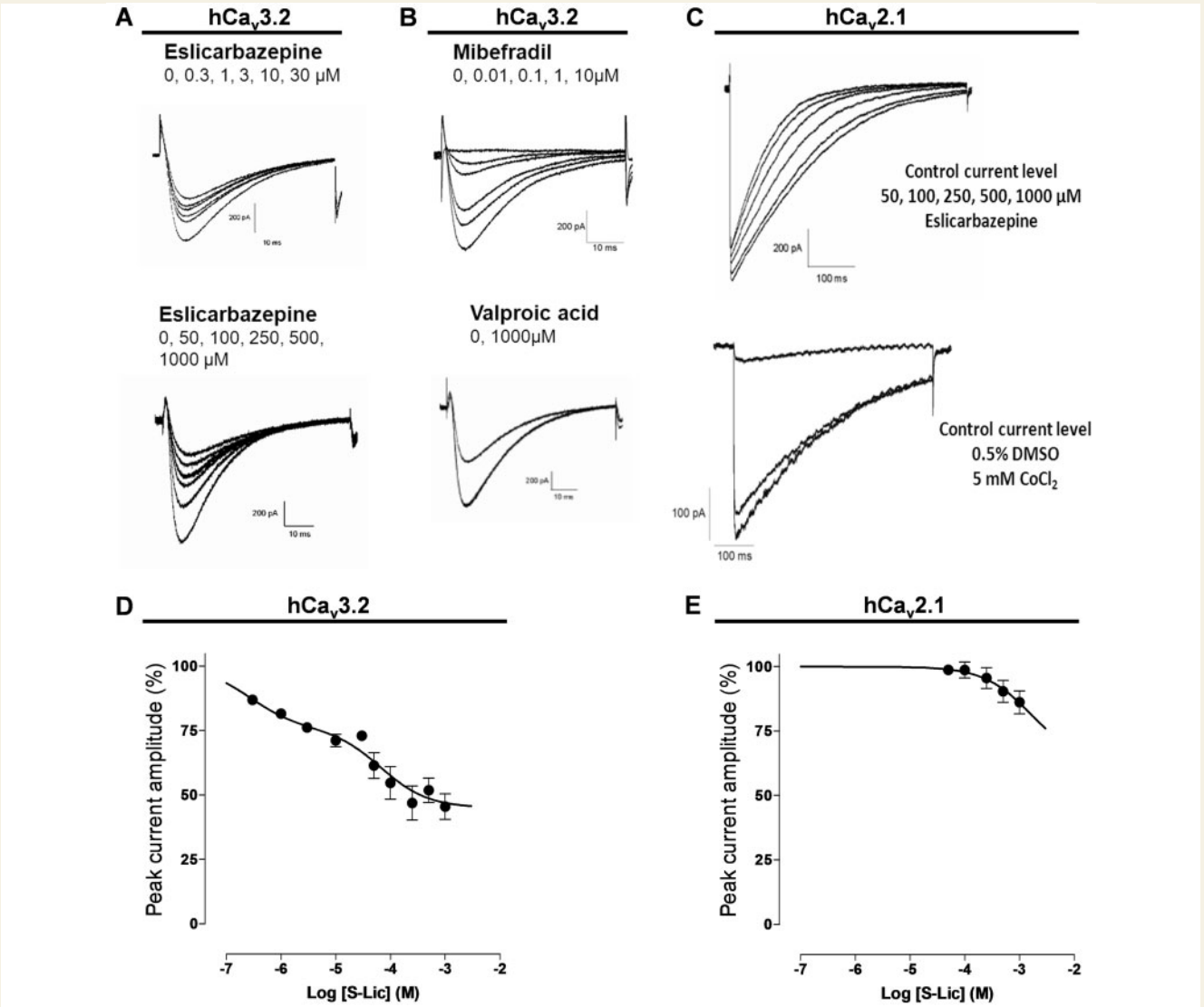

Figure 5 Effects of eslicarbazepine on $Ca_v3.2$ channels. (**A**) Analysis of $hCa_v3.2$ calcium channels stably expressed in HEK 293 cells. Depolarization from −80 to −25 mV evoked large T-type Ca^{2+} currents. Superimposed current traces with application of 0–30 µM (*top*) or 0–1000 µM eslicarbazepine (*bottom*). (**B**) $Ca_v3.2$ channels were sensitive to mibefradil, but displayed a low sensitivity to valproate. (**C**) Efficacy of eslicarbazepine on the high-threshold Ca^{2+} channel $Ca_v2.1$ expressed in CHO cells. (**D** and **E**) The dose-response relationship for $Ca_v3.2$ (**D**) or Cav2.1 (**E**) block by eslicarbazepine (S-Lic).

pharmacoresistance described for conventional drugs. In addition, the very same compound also has potent antiepileptogenic activity. Eslicarbazepine is the major active metabolite of ESL, a once-daily anticonvulsant approved in 2009 by the European Medicines Agency and more recently by the US Food and Drug Administration (FDA) as adjunctive therapy in adults with partial-onset seizures.

In our first approach, we used human tissue derived from epilepsy patients to test if eslicarbazepine is active in human epileptic specimens. In hippocampal slices from therapy-refractory epilepsy patients, seizure-like activity is largely resistant to CBZ, whereas slices from patients who are pharmacosensitive are also responsive to CBZ (Remy *et al.*, 2003*a*; Jandová *et al.*, 2006). Additionally, use-dependent block of sodium channels by CBZ is lost, whereas this is not the case in clinically responsive patients (Remy *et al.*, 2003*a*). These findings argue strongly for a change of sodium channels in the epileptic human brain that render them resistant to CBZ. In contrast, eslicarbazepine showed potent activity on sodium current recovery from inactivation and discharge behaviour. Moreover, eslicarbazepine displays add-on effects when applied in addition to CBZ in human epilepsy. In experimental epilepsy, we found that the effects of CBZ were considerably reduced in chronic epilepsy, whereas those of eslicarbazepine were not. However, we note that—in contrast to the human situation—the application of both CBZ and eslicarbazepine did not cause larger blocking effects compared to

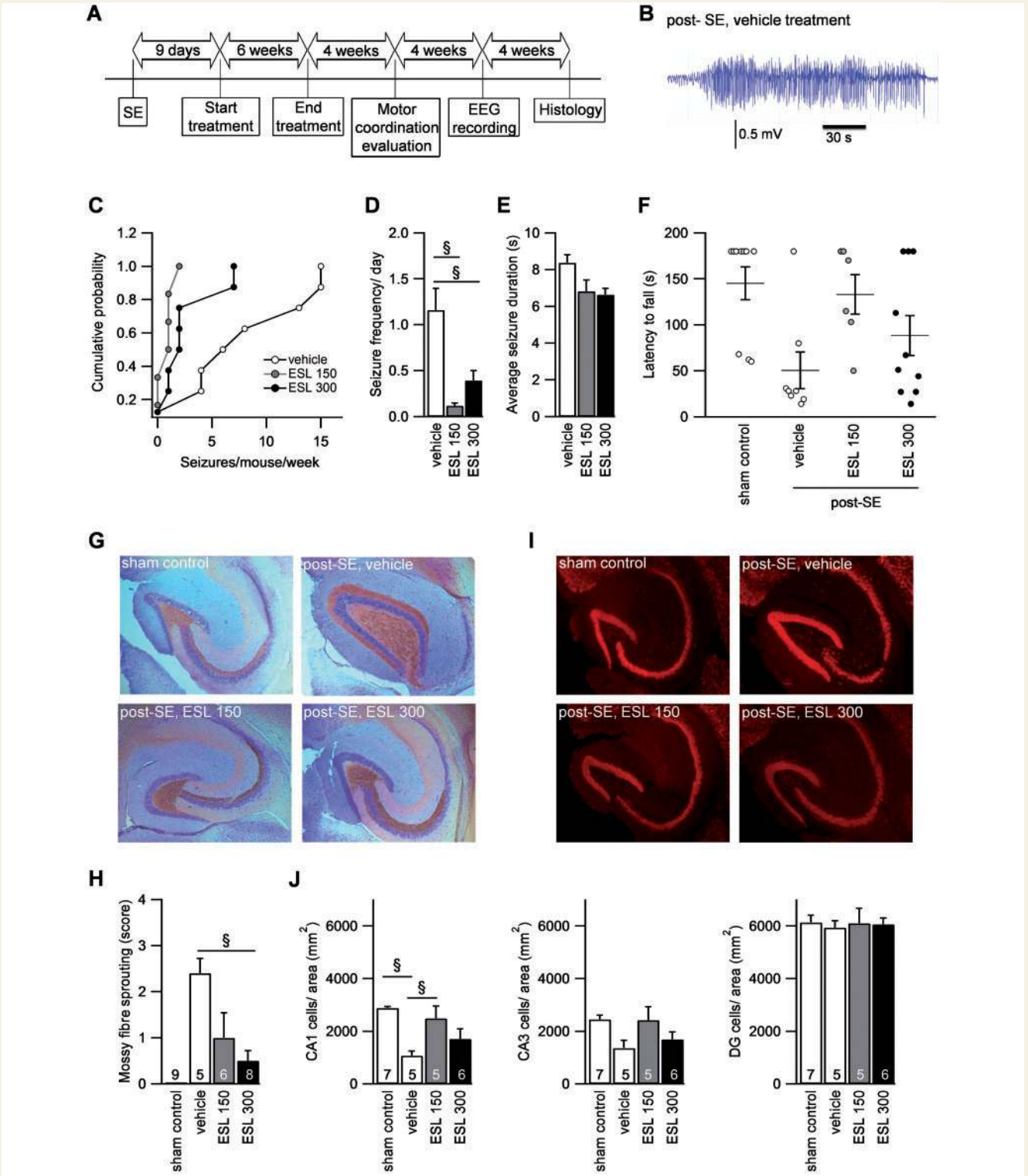

Figure 6 Antiepileptogenic effects of ESL. (**A**) Experimental schedule. Pilocarpine-treated mice were randomized and allocated to one of three treatment groups (vehicle, 150 or 300 mg/kg/day ESL, n = 8, 6, 10, respectively). Sham-control mice received only saline injections (n = 10). (**B**) Representative spontaneous electrographic seizure in a pilocarpine-treated mouse that had received vehicle. (**C** and **D**) In epileptic animals ESL treatment with both concentrations decreased electrographic seizure occurrence. §P = 0.004 and 0.021 for 150 and 300 mg/kg/day ESL, respectively. (**E**) Seizure duration was not affected by ESL treatment. (**F**) Impaired motor coordination in the Rotarod test in vehicle-treated epileptic animals is improved by 150 mg/kg/day ESL. (**G**) Timm staining reveals aberrant mossy fibre sprouting in the dentate inner molecular layer in post-status epilepticus vehicle-treated animals, which is strongly reduced by ESL treatment (*bottom*). (**H**) Quantification of Timm staining. §Significant differences, Mann-Whitney post-test with Bonferroni correction. (**I**) NeuN staining to assess neuronal loss. (**J**) Quantitative analysis of cell loss. §$P < 0.05$, Newman-Keuls post test. n-numbers for **H** and **J** are given in bars. SE = status epilepticus.

CBZ alone. The reasons for this discrepancy between human and animal model are unclear. However, our data do show that eslicarbazepine retains cellular efficacy both in chronic human and experimental epilepsy, whereas efficacy of classical anticonvulsants seems to be lost (Remy *et al.*, 2003*a*; Jandová *et al.*, 2006). In human tissue, add-on effects can be observed. This is in agreement with clinical data that suggest that ESL (and consequently eslicarbazepine) is efficacious in partial-onset seizures with or without secondary generalization (Elger *et al.*, 2007, 2009; Gil-Nagel *et al.*, 2009, 2013; Ben-Menachem *et al.*, 2010). More importantly, follow-up studies have suggested that ESL may be efficacious in patients in whom CBZ has failed (Elger *et al.*, 2007, 2009; Ben-Menachem *et al.*, 2010; Halász *et al.*, 2010). In addition to the cellular efficacy that leads to efficient inhibition of seizure activity, it is highly desirable to generate compounds that are antiepileptogenic (Pitkänen *et al.*, 2013). Transitory ESL administration after status epilepticus profoundly attenuated the development of chronic seizures, reduced behavioural deficits, and strongly reduced axonal sprouting and neuronal damage. The mechanism for this activity is unclear. However, $Ca_v3.2$ channels play a central role in the development of chronic epilepsy in this model (Su *et al.*, 2002; Becker *et al.*, 2008) and genetic deletion of $Ca_v3.2$ profoundly interferes with epileptogenesis. As we show that eslicarbazepine inhibits $Ca_v3.2$ channels at therapeutic concentrations, it is possible that $Ca_v3.2$ channel inhibition contributes to the effects of eslicarbazepine on epileptogenesis. In addition, the low toxicity shown in cultured neurons may be beneficial (Araújo *et al.*, 2004). So far, a number of experimental studies have shown positive treatment effects on epileptogenesis (Löscher and Brandt, 2010; Pitkänen, 2010; Pitkänen and Lukasiuk, 2011). However, none of those treatments has so far been brought up to the stage of clinical investigations. ESL as an approved drug would be a candidate for such clinical studies that are particularly devoted to determining antiepileptogenic effects. Taken together, these experimental results in both animal models and human epilepsy suggest that development of dual-purpose anticonvulsants that display both anticonvulsant and antiepileptogenic properties in chronic epilepsy is possible.

Funding

This work was supported by the Deutsche Forschungsgemeinschaft (SFB TR3 and SFB 1089), Nationales Genomforschungsnetzwerk NGFN^{plus} EmiNet, the BONFOR program of the University of Bonn Medical Centre, and BIAL – Portela & C^{a}, S.A.

Supplementary material

Supplementary material is available at *Brain* online.

References

Albayram O, Alferink J, Pitsch J, Piyanova A, Neitzert K, Poppensieker K, et al. Role of CB1 cannabinoid receptors on GABAergic neurons in brain aging. Proc Natl Acad Sci USA 2011; 108: 11256–61.

Araújo IM, Ambrósio AF, Leal EC, Verdasca MJ, Malva JO, Soares-da-Silva P, et al. Neurotoxicity induced by antiepileptic drugs in cultured hippocampal neurons: a comparative study between carbamazepine, oxcarbazepine, and two new putative antiepileptic drugs, BIA 2-024 and BIA 2-093. Epilepsia 2004; 45: 1498–505.

Banay-Schwartz M, Kenessey A, DeGuzman T, Lajtha A, Palkovits M. Protein content of various regions of rat brain and adult and aging human brain. Age 1992; 15: 51–4.

Becker AJ, Pitsch J, Sochivko D, Opitz T, Staniek M, Chen C-C, et al. Transcriptional upregulation of Cav3.2 mediates epileptogenesis in the pilocarpine model of epilepsy. J Neurosci Off J Soc Neurosci 2008; 28: 13341–53.

Ben-Menachem E, Gabbai AA, Hufnagel A, Maia J, Almeida L, Soares-da-Silva P. Eslicarbazepine acetate as adjunctive therapy in adult patients with partial epilepsy. Epilepsy Res 2010; 89: 278–85.

Bernard C, Anderson A, Becker A, Poolos NP, Beck H, Johnston D. Acquired dendritic channelopathy in temporal lobe epilepsy. Science 2004; 305: 532–5.

Bialer M, Soares-da-Silva P. Pharmacokinetics and drug interactions of eslicarbazepine acetate. Epilepsia 2012; 53: 935–46.

Doeser A, Soares-da-Silva P, Beck H, Uebachs M. The effects of eslicarbazepine on persistent Na(+) current and the role of the Na(+) channel β subunits. Epilepsy Res 2014; 108: 202–11.

Dunham NW, Miya TS. A note on a simple apparatus for detecting neurological deficit in rats and mice. J Am Pharm Assoc Am Pharm Assoc 1957; 46: 208–9.

Elger C, Bialer M, Cramer JA, Maia J, Almeida L, Soares-da-Silva P. Eslicarbazepine acetate: a double-blind, add-on, placebo-controlled exploratory trial in adult patients with partial-onset seizures. Epilepsia 2007; 48: 497–504.

Elger C, Halász P, Maia J, Almeida L, Soares-da-Silva P. Efficacy and safety of eslicarbazepine acetate as adjunctive treatment in adults with refractory partial-onset seizures: a randomized, double-blind, placebo-controlled, parallel-group phase III study. Epilepsia 2009; 50: 454–63.

Elger C, Bialer M, Falcão A, Vaz-da -Silva M, Nunes T, Almeida L, et al. Pharmacokinetics and tolerability of eslicarbazepine acetate and oxcarbazepine at steady state in healthy volunteers. Epilepsia 2013; 54: 1453–61.

Gil-Nagel A, Lopes-Lima J, Almeida L, Maia J, Soares-da-Silva P. Efficacy and safety of 800 and 1200 mg eslicarbazepine acetate as adjunctive treatment in adults with refractory partial-onset seizures. Acta Neurol Scand 2009; 120: 281–7.

Gil-Nagel A, Elger C, Ben-Menachem E, Halász P, Lopes-Lima J, Gabbai AA, et al. Efficacy and safety of eslicarbazepine acetate as add-on treatment in patients with focal-onset seizures: integrated analysis of pooled data from double-blind phase III clinical studies. Epilepsia 2013; 54: 98–107.

Halász P, Cramer JA, Hodoba D, Członkowska A, Guekht A, Maia J, et al. Long-term efficacy and safety of eslicarbazepine acetate: results of a 1-year open-label extension study in partial-onset seizures in adults with epilepsy. Epilepsia 2010; 51: 1963–9.

Holm IE, Geneser FA. Histochemical demonstration of zinc in the hippocampal region of the domestic pig: II. Subiculum and hippocampus. J Comp Neurol 1991; 305: 71–82.

Jandová K, Päsler D, Antonio LL, Raue C, Ji S, Njunting M, et al. Carbamazepine-resistance in the epileptic dentate gyrus of human hippocampal slices. Brain J Neurol 2006; 129: 3290–306.

Jimenez-Mateos EM, Engel T, Merino-Serrais P, McKiernan RC, Tanaka K, Mouri G, et al. Silencing microRNA-134 produces

neuroprotective and prolonged seizure-suppressive effects. Nat Med 2012; 18: 1087–94.
Köhling R. Voltage-gated sodium channels in epilepsy. Epilepsia 2002; 43: 1278–95.
Löscher W, Brandt C. Prevention or modification of epileptogenesis after brain insults: experimental approaches and translational research. Pharmacol Rev 2010; 62: 668–700.
Loureiro AI, Fernandes-Lopes C, Wright LC, Soares-da-Silva P. Development and validation of an enantioselective liquid-chromatography/tandem mass spectrometry method for the separation and quantification of eslicarbazepine acetate, eslicarbazepine, R-licarbazepine and oxcarbazepine in human plasma. J Chromatogr B Analyt Technol Biomed Life Sci 2011; 879: 2611–18.
Magistretti J, Alonso A. Biophysical properties and slow voltage-dependent inactivation of a sustained sodium current in entorhinal cortex layer-II principal neurons: a whole-cell and single-channel study. J Gen Physiol 1999; 114: 491–509.
Perucca E, Elger C, Halász P, Falcão A, Almeida L, Soares-da-Silva P. Pharmacokinetics of eslicarbazepine acetate at steady-state in adults with partial-onset seizures. Epilepsy Res 2011; 96: 132–9.
Pitkänen A. Therapeutic approaches to epileptogenesis—hope on the horizon. Epilepsia 2010; 51(Suppl 3): 2–17.
Pitkänen A, Lukasiuk K. Mechanisms of epileptogenesis and potential treatment targets. Lancet Neurol 2011; 10: 173–86.
Pitkänen A, Nehlig A, Brooks-Kayal AR, Dudek FE, Friedman D, Galanopoulou AS, et al. Issues related to development of antiepileptogenic therapies. Epilepsia 2013; 54(Suppl 4): 35–43.
Pratt JH, Berry JF, Kaye B, Goetz FC. Lipid class and fatty acid composition of rat brain and sciatic nerve in alloxan diabetes. Diabetes 1969; 18: 556–61.
Rambeck B, Jürgens UH, May TW, Pannek HW, Behne F, Ebner A, et al. Comparison of brain extracellular fluid, brain tissue, cerebrospinal fluid, and serum concentrations of antiepileptic drugs measured intraoperatively in patients with intractable epilepsy. Epilepsia 2006; 47: 681–94.
Remy S, Gabriel S, Urban BW, Dietrich D, Lehmann TN, Elger CE, et al. A novel mechanism underlying drug resistance in chronic epilepsy. Ann Neurol 2003a; 53: 469–79.
Remy S, Urban BW, Elger CE, Beck H. Anticonvulsant pharmacology of voltage-gated Na + channels in hippocampal neurons of control and chronically epileptic rats. Eur J Neurosci 2003b; 17: 2648–58.
Sekerli M, Del Negro CA, Lee RH, Butera RJ. Estimating action potential thresholds from neuronal time-series: new metrics and evaluation of methodologies. IEEE Trans Biomed Eng 2004; 51: 1665–72.
Su H, Sochivko D, Becker A, Chen J, Jiang Y, Yaari Y, et al. Upregulation of a T-type Ca2 + channel causes a long-lasting modification of neuronal firing mode after status epilepticus. J Neurosci Off J Soc Neurosci 2002; 22: 3645–55.
Tauck DL, Nadler JV. Evidence of functional mossy fiber sprouting in hippocampal formation of kainic acid-treated rats. J Neurosci Off J Soc Neurosci 1985; 5: 1016–22.
Uebachs M, Opitz T, Royeck M, Dickhof G, Horstmann M-T, Isom LL, et al. Efficacy loss of the anticonvulsant carbamazepine in mice lacking sodium channel beta subunits via paradoxical effects on persistent sodium currents. J Neurosci Off J Soc Neurosci 2010; 30: 8489–501.
Weiergräber M, Henry M, Hescheler J, Smyth N, Schneider T. Electrocorticographic and deep intracerebral EEG recording in mice using a telemetry system. Brain Res Brain Res Protoc 2005; 14: 154–64.